The thermally sensitive characteristics of a (smectic LCP/ nematic LC/chiral dopant) ternary composite system

Yang Huai; Hirokaku Yamane; Hirotsuku Kikuchi; Zhang Guo; Chen Xinfang; Tisato Kajiyama

PLEASE SCROLL DOWN FOR ARTICLE

The thermally sensitive characteristics of a (smectic LCP/ nematic LC/chiral dopant) ternary composite system

by YANG HUAI*†, HIROKAKU YAMANE‡, HIROTSUKU KIKUCHI‡, ZHANG GUO†, CHEN XINFANG† and TISATO KAJIYAMA‡

†Institute of Materials Science, Jilin University, Changchun, 130023, China
‡Department of Chemical Science and Technology, Faculty of Engineering, Kyushu University, 6-10-1 Hakozaki, Higashi-ku, Fukuoka 812, Japan

A transition between the transparent smectic A (SmA) phase and the light scattering chiral nematic (N*) phase was realized based on the thermally induced SmA ↔ N* phase transition for the homeotropically aligned [liquid crystalline polymer (LCP)/liquid crystal (LC)/chiral dopant] ternary composite system. The LCP played an important role in increasing the intensity of the light scattering of the heat-induced N* phase. Meanwhile the effects of the composition of the ternary composite system on the thermo-optical characteristics were also investigated.

1. Introduction

It is understood that a sharp change in the helical pitch from a certain value to infinity within a tiny temperature range occurs just above the N* → SmA phase transition in a liquid crystal (LC) in which a SmA phase exists below the N* range [1]. Qualitatively, this effect can be explained as follows: due to the relatively high rigidity, it is difficult for the layer structure of the SmA phase to buckle in order to twist. On cooling from the N* to the SmA phase and near the N* → SmA phase transition temperature, the molecules start to form smectic-like short-range ordering to some degree, and some groups of molecules begin to show some fleeting layer structure. As the temperature drops closer to the transition, the size of the groups of molecules gets larger and the smectic-like short-range ordering increases. This results in the twisting elastic constant tending to infinity and the untwisting of the helix of the N* phase. Since all this can only take place very near the N* → SmA transition temperature, the pitch change happens within a tiny temperature range just above the transition. Then, if a cell sandwiching the LC is treated homeotropically, it is possible that a sharp change in transmittance from a light-scattering state to a transparent one on cooling, or from a transparent state to a light scattering one on heating, should occur for the cell accompanied with the drastic change in the pitch, since an N* and S$_A$ phase are light scattering and transparent in this kind of orientation, respectively. Thus, it is the purpose of this paper to investigate the effects of the ratios of the liquid crystalline polymer (LCP) and the chiral dopant on the thermally sensitive thermo-optical characteristics based on the SmA ↔ N* phase transition for the homeotropically aligned (smectic LCP/nematic LC/chiral dopant) ternary composite system, about which little has been reported to our knowledge.

2. Experimental

A side-chain liquid crystalline copolymer exhibiting a SmA mesophase designated by the name of PS(4BC/DM), the commercially available nematic LC, E7 (Merck) and the commercially available chiral compound, CB-15 (Merck), were used as the three components of the (smectic LCP/nematic LC/chiral dopant) ternary composite system. In order to compare the thermo-optical characteristics of the [PS(4BC/DM)/ E7/CB-15] ternary composite system with those of a [low molecular weight smectic A liquid crystal (LMWSmALC)/E7/CB-15] ternary composite system, the commercially available LMWSmALC, S2 (Merck), was used as the LMWSmALC component. The chemical structures and some physical parameters of the four materials are shown in figure 1. PS(4BC/DM) was synthesized following the method proposed by Finkelmann *et al.* [2]. The purity and molecular weights of PS(4BC/DM) were evaluated by GPC, and the block ratio determined by NMR and IR spectroscopies. Meanwhile, the phase transition behaviour and aggregate states were determined by POM observation, DSC and WAXD measurements. The [PS(4BCDM)/E7/CB-15]

*Author for correspondence.

(1) Liquid crystalline copolymer

PS(4BC/DM) ($n=12$ $m=4$; $n=x+y=12$; $x/y=52 \cdot 5/47 \cdot 5$)

$M_n=8000$; $M_w=10270$; $M_w/M_n=1 \cdot 28$

SmA 337 I ($T_g=254$ K)

(2) Low molecular weight liquid crystal E7 (mixture of liquid crystals with positive dielectric anisotropy, Cr 263 N 333 I.

(3) Chiral dopant CB-15 right-handed helix $[\alpha]_D^{20}=+13°$; Cr 277 Ch(247) I.

(4) Low molecular weight liquid crystal S2 (mixture of liquid crystals with positive dielectric anisotropy); Cr 272·2 SmA 321·2 N 322·2 I.
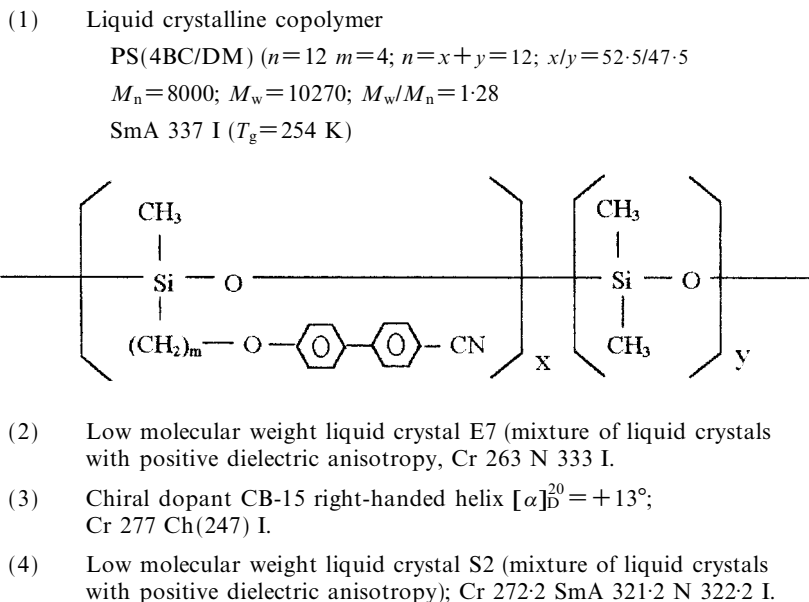
Figure 1. The chemical structure and parameters of the materials used.

and (S2/E7/CB-15) composites were prepared by a solvent cast method from an acetone solution.

The phase transition behaviour and aggregate states of the composites were investigated on the basis of differential scanning calorimetry (DSC), polarizing optical microscopy (POM) and X-ray diffraction studies (WAXD and SAXS). The DSC thermograms were obtained using a Rigaku DSC 8230B at a heating rate of $5 \cdot 0$ K min^{-1} under the protection of a dry nitrogen purge, the POM microphotographs were taken under crossed Nicols using a Nikon polarizing optical microscope, and the WAXD and SAXS studies carried out using Ni filtered ($\lambda = 1 \cdot 5405$ Å) radiation from M18XHF (Macscience) and RU-300 (Rigaku) X-ray generators, respectively.

The method proposed by Kahn [3] was used to obtain the homeotropic alignment. A 14-μm-thick PET

film was used as the spacer of the cell made from ITO substrates and the composites were filled into the cells by capillary action in the isotropic (I) phase. The Cano wedge technique [4] was used to measure the pitch lengths of the N* phases and the rubbed PVA film was used to obtain the planar alignment. Each sample was first heated to a temperature of 2 K below the N*→I phase transition temperature and then the pitch was measured on cooling at a rate of 0·5 K min^{-1}.

The measurement of the dependence of the transmittances of the cells sandwiching the composites on temperature were carried out with the instrument, as schematically shown in figure 2. A He–Ne laser (2 mW, 632·8 nm) was used to provide the incident beam and the values were recorded by the photodiode. In this experiment, the transmittance of a blank cell was taken as 100 per cent.

3. Results and discussion

3.1. *The phase transition behaviour and aggregate structures of the ternary composite systems*

On the basis of POM observation, DSC, WAXD and SAXS measurements, the phase diagrams of two [PS(4BC/DM)/E7/CB-15] ternary composite systems, named as systems **A** and **B**, in which CB-15 ratios were fixed at 2·4 wt % and 4·8 wt %, were determined as shown in figures 3 and 4, respectively. It can be noted from these two phase diagrams that a SmA phase existed below the N* phase in both systems when the PS(4BC/DM) ratio was between 19·5 and 43·9 wt % for system **A**, and between 23·8 and 47·6 wt % for system **B**,
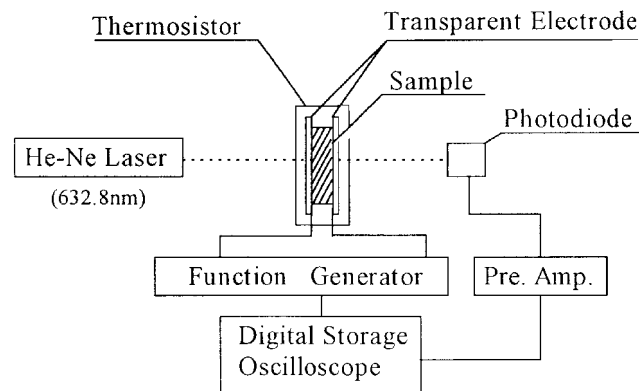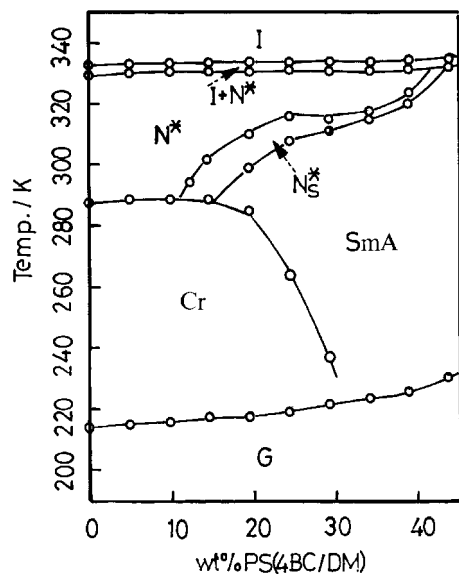

Figure 2. Schematic representation of the instrument used to measure the thermo-optical characteristics of the ternary composite system.

Figure 3. The phase diagram of the ternary composite system **A**. I=isotropic; N*=chiral nematic; N_s^*=smectic-like short-range ordering; SmA=smectic A; Cr=crystalline; G=glassy.

Figure 4. As for figure 3, but for system **B**.

respectively. The SmA → N* phase transition temperatures in both systems increase with increasing PS(4BC/DM) ratio. Furthermore, in both systems, smectic-like short-range ordering exists in a temperature range just above the transition. At first, the temperature range of the ordering becomes narrower as the PS(4BC/DM) ratio increases, because the transition becomes more first order as the N* range decreases [5]. Then, the temperature range of the ordering becomes somewhat wider, with the ratio increasing continually in the higher PS(4BC/DM) ratio region near the SmA–N*–I tricritical point, since the molecular chirality causes the ordering to increase near the tricritical point [1]. Besides these, X-ray measurements have proved that the ordering increases as the temperature decreases near to the N* → SmA phase transition.

Figures 5 and 6 show the temperature dependences of the helical pitches of the samples of systems **A** and **B**, respectively. In spite of the effect of the PS(4BC/DM) ratio on the pitch in either system, which will be discussed in another paper, it can be seen that, when a N* phase is transformed into a SmA phase, as mentioned in the Introduction, the helical pitch changes from a value of the order of a few μm to infinity within a tiny temperature range for each sample of the ternary composite system studied. In addition, the helical pitch decreases with increasing ratio, i.e. the helical twisting power increases as the CB-15 ratio increases, obeying the common law.
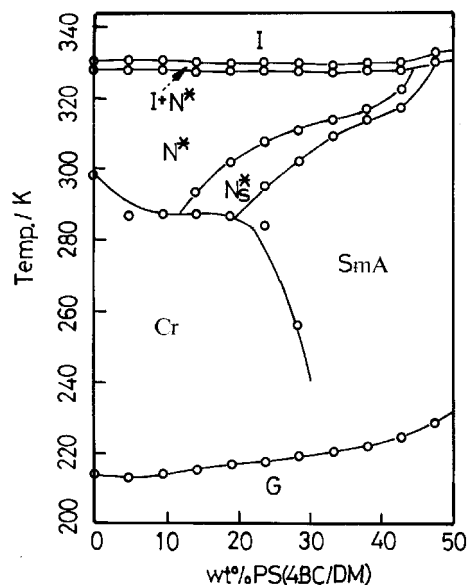
3.2. The thermally sensitive thermo-optical characteristics of the ternary composite systems

Tables 1 and 2 list the weight ratios of PS(4BC/DM)/E7/CB-15 in the samples of systems **A** and **B**, and the thicknesses of the corresponding cells sandwiching these samples, where the inner surfaces had been treated homeotropically, respectively. Before the thermo-optical characteristics of each cell were measured, the cell was first heated to the I phase and then cooled at a rate of 0·5 K min^{-1} to the SmA phase. Thus, the homeotropically aligned SmA phase was formed by the anchoring effect of the surface orientation agent. Figure 7 shows the temperature dependence of the transmittances of the cells containing samples **A1**–**A5** on heating and cooling at different rates, and figure 8 those of samples **B1**–**B5** in the sequence.

It can be seen from these figures that the change from a transparent state to a light scattering one based on the SmA → N* phase transition takes place in all samples of systems **A** and **B** on heating. The temperature interval for the transmittance going from 10 to 90 per cent response increases with PS(4BC/DM) increasing in either system. This should stem from the increasing viscosity of the system as the ratio increases. Meanwhile the temperature interval decreases as the CB-15 ratio increases for the sample with the same relative ratio of PS(4BC/DM)/E7 when systems **A** and **B** are compared. This obviously originates from the fact that the helical twisting power of the N* phase increases with increasing CB-15 ratio. It can be seen that the changes are rather sharp for the samples of system **B**. For example, the temperature interval for the transmittance going from
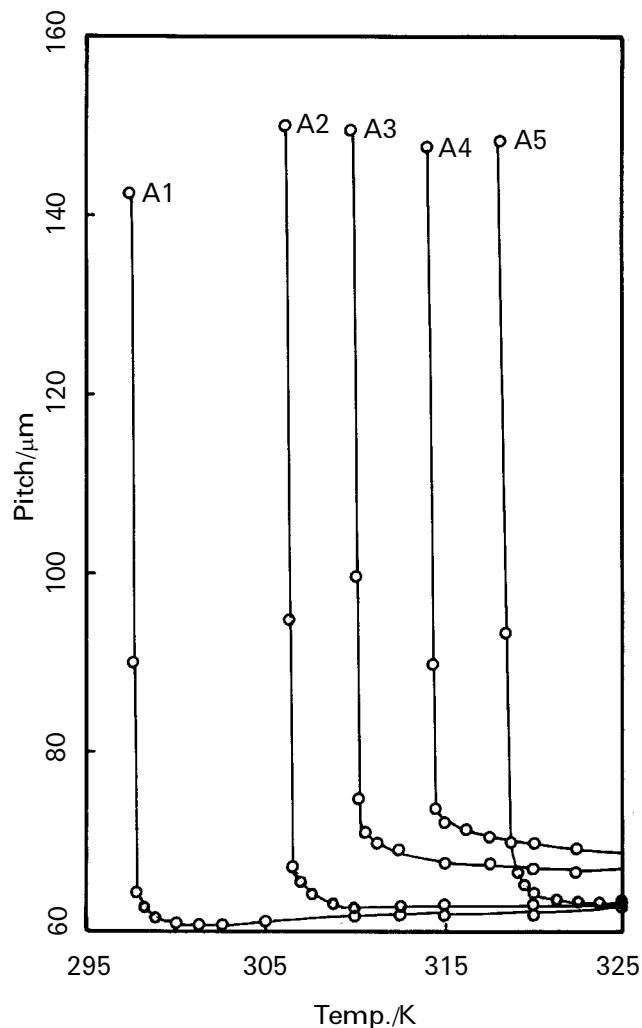
Figure 5.   The temperature dependence of the pitches of the N* phases of samples **A1**–**A5**.

Figure 6.   As for figure 5, but for samples **B1**–**B5**.

10 to 90 per cent response is no greater than 0·5 K for sample **B1** and is only about 1·0 K for sample **B5** when observed from the curves measured at a heating rate of 10·0 K min^{-1} [figure 8(*a*) and 8(*e*), respectively]. The effects of the ratios of PS(4BC/DM) and CB-15 on the responses of the SmA → N* phase transition can be seen further, in detail, from the times necessary for the change in the transmittances on going from 10 to 90 per cent response for the samples of these two systems measured at different heating rates (table 3). For the same reason as the effect of the ratios of PS(4BC/DM) and CB-15 on the temperature interval necessary for the trans- mittance going from 10 to 90 per cent response, the time necessary for the change in the transmittance going from 10 to 90 per cent response increases as the PS(4BC/DM) ratio increases for either system and decreases as the CB-15 ratio increases for the samples with the same ratio of PS(4BC/DM)/E7.
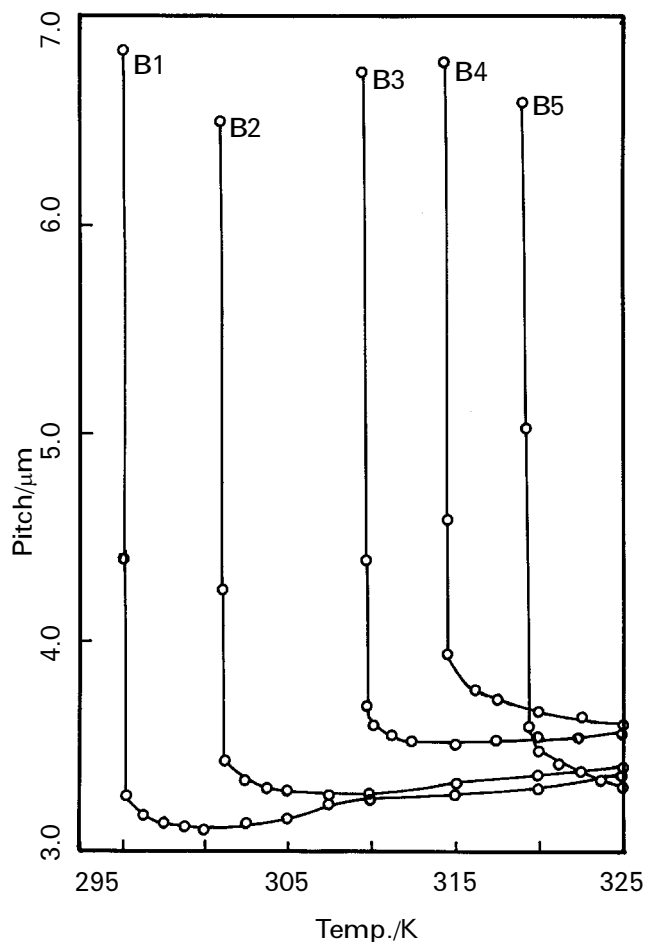
It is also shown in figure 7(*a*) and 7(*b*), and figure 8(*a*) and 8(*b*) that the intensities of the light scattering of the N* phases decrease with increasing temperature. It is assumed that the helices of the small domains in the N* phases in the centre of the cells tend to rotate from a direction parallel to the substrate surfaces to an oblique or perpendicular direction to them, in order to be in a lower energy state [6, 7]. It is a natural result that this tendency increases with increasing temperature since the motion of the molecules aggravates with increasing temperature. This results in increased transmittances of the N* phase of samples **A1**, **A2**, **B1**, and **B2** with increasing temperature. However the tendency of the transmittance of the N* phase to increase with increasing temperature lessens with the increasing PS(4BC/DM) ratio for either system, and stable, strong light scattering N* phases have been obtained for samples **A3**–**A5** and **B3**–**B5**. Considering the conformation of the backbones of an LCP in the SmA phase, we can give a possible explanation. In the homeotropically aligned SmA phase, the backbones of the PS(4BC/DM) system have been

oriented with the plane containing them parallel to the substrate surfaces. This kind of orientation of the backbones can be retained in the heat-induced N* phase to some degree due to the fact that the formation of a helix does not require a great rearrangement of the polymer backbones, because of the very small change in the twist angles of the mesogenic molecules when considering the structures of the SmA and N* phases. This results in the rotation of the helices of the small domains in the N* phase in the centre of the cell from a direction parallel to the substrate surfaces to an oblique or perpendicular orientation to them, and being in a lower energy state becomes difficult with increasing ratio. Therefore, the intensity of light scattering of the N* phase over the entire temperature range of the N* phase becomes more stable with increasing ratio in either system. However, after observing figure 7 and figure 8 carefully, it is found that for samples with the same ratio of PS(4BC/DM)/E7, the minima of transmittances of the N* phases of the samples of system **A** are, on the whole, somewhat greater than those of system **B**. This should be attributed to the longer pitches of the samples of system **A** than those of the samples of system **B**. It is necessary to mention that it had been proved that, because the helices of the small domains in the N* phase in the centre of the cell with a homeotropic boundary condition tend to be oblique or perpendicular to the substrate surfaces, and to be in a lower energy state, the cell was rather clear when a LMWN*LC was sandwiched in a cell with homeotropic boundary condition [6, 8]. Therefore, when a LMWLC was sandwiched in a cell with homeotropic boundary condition and heated from the SmA to the N* phase, the contrast ratio between the SmA phase and the N* phase was very low, usually not over 3∶1, which was also indicated in some experiments such as those performed by Sasaki *et al.* [9]. This was further demonstrated by our own experiment. Figure 9 shows the dependence of the transmittances of the homeotropically aligned (S2/E7/CB-15) ternary composites with temperature on heating. Comparing the two parts of the figure with samples **B1**–**B5**, it can be seen that, although the

pitch lengths of these two samples and the thicknesses of the cells containing them are comparable with those of the samples of system **B**, the transmittances of the N* phase of these two samples are much higher than those of samples of system **B** (on the whole). This indicates that the LCP, PS(4BC/DM), has played an important role in increasing the intensities of the light scattering of the N* phase of the [PS(4BC/DM)/E7/CB-15) ternary composite system.

From figures 7 and 8, it can be seen that the initially homeotropic SmA phase can be obtained again by the anchoring effect of the surface orientation agent when each sample is cooled at a slow enough rate from the N* phase. However, if the cooling rate is fast enough, a light scattering SmA phase forms. This is because, if the cooling rate is rapid enough, there is not enough time for the completion of the rearrangement of the molecules from the N* phase into the homeotropically aligned SmA phase and the molecules will be frozen in the high viscous SmA phase. Thus, a focal conic texture forms in the SmA phase which scatters light. Table 4 lists the transmittances of the resulting SmA phases of the samples of the two systems obtained on cooling from the corresponding N* phases at different cooling rates. From these data and figures 7 and 8, it is known that the transmittances of the resulting SmA phases of the samples of systems **A** and **B** increase with decreasing PS(4BC/DM) ratio at a certain cooling rate. This is because, on the one hand, the viscosity of either system decreases with decreasing ratio, and on the other hand, the N* → SmA phase transition tends to be more second order in character. Comparing systems **A** and **B** with each other, it is shown that, if the cooling rate is the same, for the samples with the same relative ratio of PS(4BC/DM)/E7, the greater the CB-15 ratio, the lower the transmittance of the resulting SmA phase. This should also result from the rearrangement of the molecules from the N* phase to the homeotropic SmA phase becoming more difficult with increasing CB-15 ratio, i.e. with the helical twisting power of the N* phase increasing. Moreover, the transmittances of the resulting SmA

Table 1. The ratios of PS(4BC/DM)/E7/CB-15 of the samples of system **A** and the thicknesses of the corresponding cells containing these samples.

Sample	**A1**	**A2**	**A3**	**A4**	**A5**
Ratio/wt %	19·5/78·1/2·4	24·4/73·2/2·4	29·3/68·3/2·4	34·2/63·4/2·4	39·0/58·6/2·4
Thickness/μm	14	17	16	16	14

Table 2. As for table 1 but for the samples of system **B**.

Sample	**B1**	**B2**	**B3**	**B4**	**B5**
Ratio/wt %	23·8/71·4/4·8	28·6/66·6/4·8	33·3/61·9/4·8	38·1/57·1/4·8	42·9/52·3/4·8
Thickness/μm	23	20	18	17	16
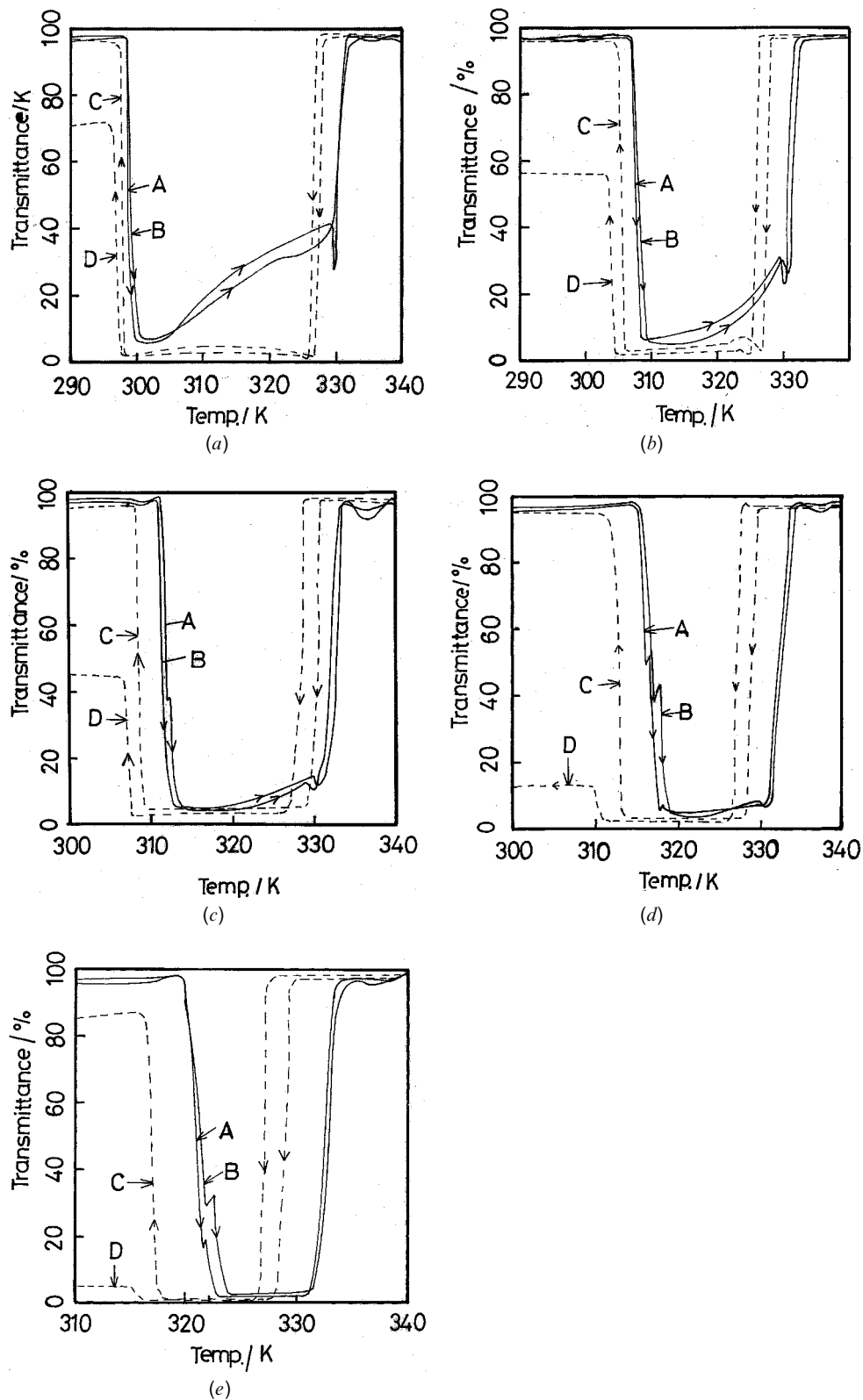
Figure 7.   The dependence of the transmittance of the cell for each sample against temperature. *A*: at a heating rate of 10·0 K min^{-1}; *B*: at a heating rate of 30·0 K min^{-1}; *C*: at a cooling rate of 1·0 K min^{-1}. *D*: at a cooling rate of 5·0 K min^{-1}. (*a*) Sample **A1**; (*b*) Sample **A2**; (*c*) Sample **A3**; (*d*) Sample **A4**; (*e*) Sample **A5**.

Figure 8.   As for figure 7. (*a*) Sample **B1**; (*b*) Sample **B2**; (*c*) Sample **B3**; (*d*) Sample **B4**; (*e*) Sample **B5**.

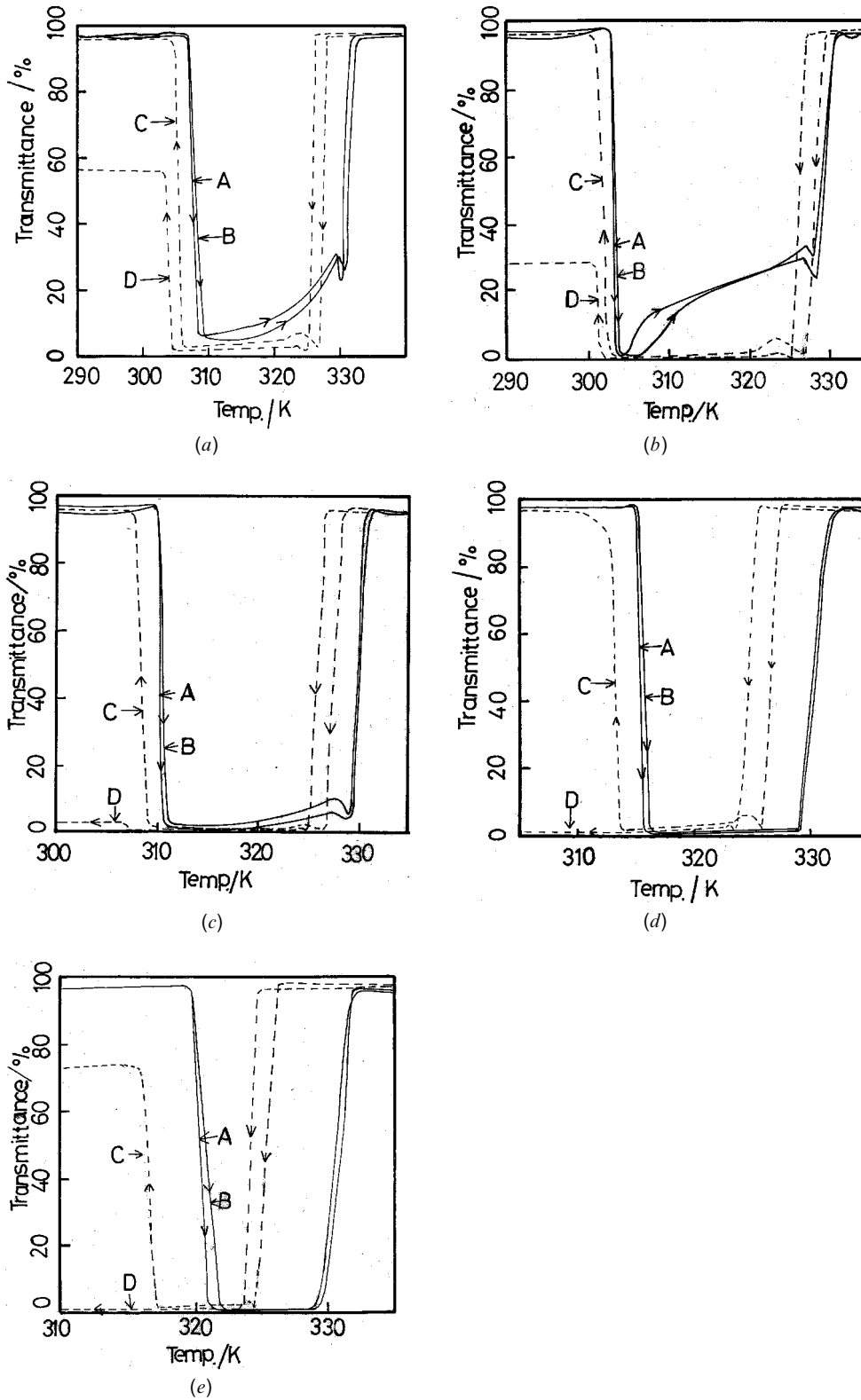Table 3. The times necessary for the sharp change in the transmittance of the samples on going from 10 to 90 per cent response at different heating rates.

	Sample									
	A1	A2	A3	A4	A5	B1	B2	B3	B4	B5
Heating rate/K min^{-1}	Time/s									
10·0	5·4	7·8	9·4	10·8	13·2	2·1	3·0	3·9	5·0	7·5
30·0	3·4	3·9	4·6	5·3	6·4	0·9	1·2	1·8	2·6	4·0

Table 4. The transmittances of the resulting SmA phases obtained on cooling from the corresponding N* phase at different cooling rates.

	Sample									
	A1	A2	A3	A4	A5	B1	B2	B3	B4	B5
Cooling rate/K min^{-1}	Transmittance/%									
0·5	97·0	97·9	97·2	97·0	94·8	98·0	97·0	97·6	97·1	94·0
1·0	97·0	96·0	95·3	95·6	85·2	95·7	96·8	96·0	96·5	72·7
5·0	70·9	56·0	45·0	12·8	5·0	52·0	29·0	2·6	1·0	0·8
10·0	32·0	28·1	16·5	4·4	2·3	12·8	5·6	1·2	0·8	0·7

phases over 90 per cent for all samples of the two systems can only be reobtained on a cooling rate below 1·0 K min^{-1}. After the curves measured on cooling at a rate of 1·0 K min^{-1} are observed carefully, it is found that the response time for the change from the light scattering N* phase to the transparent SmA phase going from 10 to 90 per cent response also increases with increasing PS(4BC/DM) ratio for either system and increases with increasing CB-15 ratio for the samples with the same relative ratio of PS(4BC/DM)/E7 in systems **A** and **B**. This is clearly also because the viscosity of the system increases with increasing PS(4BC/DM) ratio and the helical twisting power of the N* phase increases with increasing CB-15 ratio. In addition, thermal hysteresis at the transition from the light-scattering state to the transparent state has appeared in each sample compared with the heating course, and the thermal hysteresis increases as the PS(4BC/DM) ratio increases, on the whole, for either system (figures 7 and 8). In order to better explain this phenomenon, the SmA → N* and N* → SmA phase transition temper-

atures of these samples, denoted as T_{mh} and T_{mc}, were measured by DSC on heating and cooling at a rate of 1·0 K min^{-1}, respectively. The phase transition temperatures measured are listed in table 5, except for sample **B1**, because its SmA ↔ N* phase transition temperatures could not be observed accurately on the DSC because the latent heats were too small. The temperatures at which the transitions from the light-scattering state to the transparent state began, denoted as T_c, (figures 7 and 8) are also listed in table 5. It can be seen from the data of samples of system **B** that, for a sample **Bi**, $T_{mh}i$ is greater than $T_{mc}i$. This shows that the thermal hysteresis at the N* → SmA phase transition on cooling really exists. Moreover, the difference of $T_{mh}i - T_{mc}i$, i.e. the thermal hysteresis, increases as the N* range decreases on the whole. This should again result from the N* → SmA phase transition becoming more first order as the N* range decreases (on the whole). Thus, the smectic-like short-range ordering decreases and the twisting elastic constant tends to be less infinite as the width of the N* phase decreases for

Table 5. The values of T_{mh}, T_{me} and T_c of the different samples.

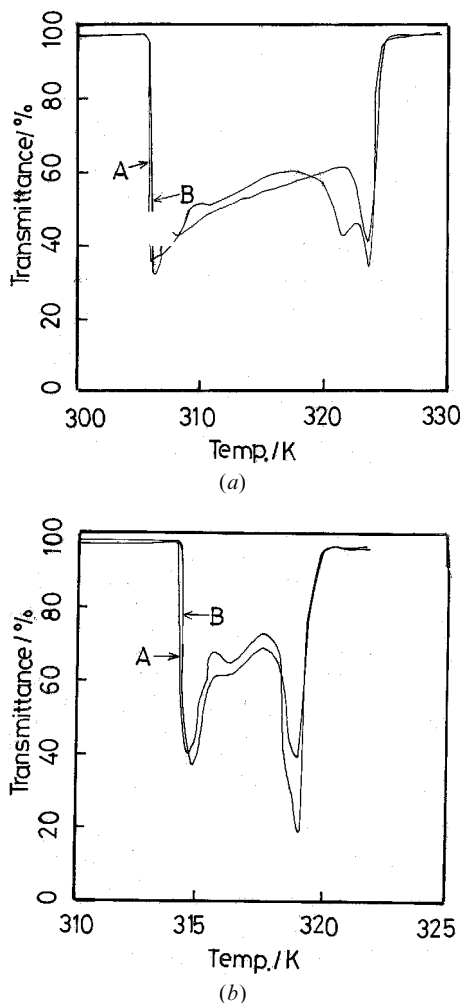|	Sample								
Transition	A1	A2	A3	A4	A5	B2	B3	B4	B5
T_{mh}/K	298·4	306·6	309·8	314·3	319·1	303·2	309·8	314·7	318·9
T_{me}/K	298·2	306·2	309·4	313·4	318·5	303·1	309·4	314·1	318·3
T_e/K	298·0	306·0	309·0	313·1	317·5	302·9	309·0	313·6	317·3

Figure 9. (*a*) The dependence of the transmittance of the cell with a homeotropic boundary condition containing the (S2/E7/CB-15) ternary composite (S2: E7: CB-15 = 61·9 wt %: 33·3 wt %: 4·8 wt %) against temperature. *A*: at a heating rate of 10·0 K min^{-1}; *B*: at a heating rate of 30·0 K min^{-1}. (For this sample, $T_{N^* \to I} = 323·8$ K, $T_{SmA-N^*} = 305·7$ K; the thickness of the cell and the pitch length of the N* phase are 18 μm and 3·4 μm, respectively, and it had been observed that the pitch length changed little with temperature in the entire temperature range of the N* phase.) (*b*) As for figure 9 (*a*) but for the sample with S2: E7: CB-15 = 85·7 wt %: 9·5 wt %: 4·8 wt %. (For this sample, $T_{N^* \to I} = 320·1$ K, $T_{SmA-N^*} = 314·1$ K; the thickness of the cell and the pitch length of the N* phase are 19 μm and 3·9 μm, respectively, and it had also been observed that the pitch length changed little with temperature in the entire temperature range of the N* phase.)

the system when the temperature decreases closer to the N* → SmA phase transition. Furthermore, the difference in $T_c i - T_{mc} i$ increases with increasing PS(4BC/DM) ratio. This indicates that the thermal hysteresis at the transition from a light scattering state to a transparent one in each sample is also influenced by the

PS(4BC/DM) ratio. A possible explanation is that the viscosity of a sample increases with increasing PS(4BC/DM) ratio and this results in a little hysteresis of the rearrangement of the molecules from a light-scattering state to a homeotropically-aligned SmA phase relative to the N* → SmA transition. Thus, resulting from two aspects: on the one hand, the N* → SmA transition is becoming more first order with decreasing N* range and on the other hand, the viscosity of the sample increases with increasing PS(4BC/DM) ratio, the thermal hysteresis at the transition from a light-scattering state to the transparent state increases with increasing PS(4BC/DM). However, this explanation is only approximately suitable for the samples of system **A**. Perhaps it is because the difference among the measured temperatures, T_{mh}, T_{mc} and T_c, is small and they cannot be measured very accurately due to the existence of the error of the instruments used. Since the hysteresis in the rearrangement of the molecules from a light-scattering state to a homeotropically aligned SmA state exists, it is easily understood that the thermal hysteresis at the transition from a light scattering state to a transparent SmA state for a sample increases a little with increasing cooling rate. This explanation is still somewhat speculative. Therefore, the thermal hysteresis at the transition from a light scattering state to a transparent state is to be investigated further.

4. Conclusions

From our own and other experiments, it is known that although a transition from a SmA to a N* phase is easily found in a LMWLC, or a mixture of a LMWLC and a chiral dopant in which the SmA phase exists below the N* range, the contrast ratios between the SmA and the N* phase are very low if the LC is sandwiched homeotropically in the cell, and heated from the SmA to the N* phase, since the helices of the small domains of the N* phase in the centre of the cell tend to be oblique or even perpendicular to the substrate surfaces. However, it was revealed by us that the contrast ratio can be improved greatly by using a homeotropically-aligned (smectic LCP/nematic LC/chiral dopant) ternary composite system because the backbones of the LCP, which have been oriented anisotropically somewhat in the homeotropic SmA phase, have a restricting effect on the rotation of the helices of the small domains of the heat-induced N* phase. Moreover, the response time necessary for the change from the transparent to the light-scattering states on heating increases, and decreases with increasing ratios of PS(4BC/DM) and CB-15, respectively, while the response time necessary for the change from the light scattering state to the transparent state on cooling increases with the two ratios increasing. In addition, a SmA phase with high

transmittance is easier to form on cooling from the corresponding N* phase as the ratios of PS(4BC/DM) and CB-15, and the cooling rate decrease. Otherwise, a light-scattering SmA phase forms easily. Thus, based on the above characteristics, by adjusting the composition of the ternary composite system, a thermo-optical effect with respect to the rapid response, high contrast and the bistable reversibility can be realized.

It is possible for this system to be used as a thermo-optical sensor. It is also possible for it to be used as a thermal addressing liquid crystal display material for which the light-scattering texture is induced based on the SmA → N* phase transition, differing from a conventional thermal addressing liquid crystal display material when a SmALC or a N*LC is used for which the light-scattering texture is induced based on mesophase → I → mesophase transitions. The difference in response times, contrast ratios and solutions when the former and

latter are used as thermal addressing liquid crystal display materials will be discussed in the near future.

References

[1] LUBENSKY, T. C., 1975, *J. de Phys.*, **36,** C1–151.
[2] FINKELMANN, H., KIECHLE, U., and REHAGE, G., 1983, *Mol. Cryst. liq. Cryst.*, **94,** 343.
[3] KAHN, F. J., 1973, *Appl. Phys. Lett.*, **22,** 386.
[4] CANO, R., 1968, *Bull. Soc. Franc. Mineral.*, **91,** 20.
[5] CLADIS, P. E., and TORZA, S., 1975, *J. Appl. Phys.*, **2,** 584.
[6] KASHNOW, R. A., BIGELOW, J. E., COLE, H. S., and STEIN, C. R., 1974, *Liquid Crystals and Ordered Fluids*, edited by J. F. Johnson and R. S. Porter (New York: Plenum Press), Vol. 2, p. 483.
[7] CLADIS, P. E., and KLEMAN, M., 1972, *Mol. Cryst. liq. Cryst.*, **16,** 1.
[8] KAWACHI, M., KATO, K., and KOGURE, O., 1977, *Japan J. Appl. Phys.*, **16,** 1263.
[9] SASAKI, A., KURAHASHI, K., and TAKAGI, T., 1974, *J. appl. Phys.*, **45,** 4356.